IOP Publishing Nanotechnology
Nanotechnology **25** (2014) 185701 (8pp) doi:10.1088/0957-4484/25/18/185701

Vibrational and thermodynamic properties of α-, β-, γ-, and 6, 6, 12-graphyne structures

Nihan Kosku Perkgöz[1,2] **and Cem Sevik**[3]

[1] Department of Electrical and Electronics Engineering, Faculty of Engineering, Anadolu University, Eskisehir, TR 26555, Turkey
[2] UNAM-National Nanotechnology Research Center, Bilkent University, Ankara 06800, Turkey
[3] Department of Mechanical Engineering, Faculty of Engineering, Anadolu University, Eskisehir, TR 26555, Turkey

E-mail: nkperkgoz@anadolu.edu.tr and csevik@anadolu.edu.tr

Received 7 January 2014, revised 26 February 2014
Accepted for publication 3 March 2014
Published 15 April 2014

Abstract

Electronic, vibrational, and thermodynamic properties of different graphyne structures, namely α-, β-, γ-, and 6, 6, 12-graphyne, are investigated through first principles–based quasi-harmonic approximation by using phonon dispersions predicted from density-functional perturbation theory. Similar to graphene, graphyne was shown to exhibit a structure with extraordinary electronic features, mechanical hardness, thermal resistance, and very high conductivity from different calculation methods. Hence, characterizing its phonon dispersions and vibrational and thermodynamic properties in a systematic way is of great importance for both understanding its fundamental molecular properties and also figuring out its phase stability issues at different temperatures. Thus, in this research work, thermodynamic stability of different graphyne allotropes is assessed by investigating vibrational properties, lattice thermal expansion coefficients, and Gibbs free energy. According to our results, although the imaginary vibrational frequencies exist for β-graphyne, there is no such a negative behavior for α-, γ-, and 6, 6, 12 -graphyne structures. In general, the Grüneisen parameters and linear thermal expansion coefficients of these structures are calculated to be rather more negative when compared to those of the graphene structure. In addition, the predicted difference between the binding energies per atom for the structures of graphene and graphyne points out that graphyne networks have relatively lower phase stability in comparison with the graphene structures.

S Online supplementary data available from stacks.iop.org/nano/25/185701/mmedia

Keywords: thermal expansion coefficient, graphene, graphyne, quasi harmonic theory

(Some figures may appear in colour only in the online journal)

1. Introduction

Graphene has generated great interest since its first isolation by Novoselov *et al* due to its superior properties, including robustness, stability, flexibility, and thermal and electrical conductivity [1, 2]. These features indicate its high potential to be used for numerous applications—specifically, in the fields of electronics, photonics, and optoelectronics [3–5]. With such a motivation, researchers have pursued different techniques of controlling the properties of graphene, including intentionally introducing defects, strains, and dopants, as well as employing different methods of chemical functionalization [4, 6, 7]. Regarding these techniques, the material properties have not been sufficiently optimized to be used in practical applications. Therefore, interest in its allotropes has grown significantly owing to the expected extraordinary properties [8, 9].

Among these materials, graphyne—composed of one-atom-thick sheets of carbon atoms but containing sp carbon

bonds in addition to sp^2 hybridized bonds—has garnered considerable attention. Possible alterations in the bonds allow for the formation of different structures, which can lead to unforeseen changes in the material properties. One of the graphyne forms, 6, 6, 12-graphyne, has grabbed attention for its peculiar properties such as direction-dependent conductivity and two self-doped nonequivalent distorted Dirac cones functionalities [10]. Also, γ-graphyne, which was found to have a direct energy bandgap [11, 12], is appealing for bandgap engineering in the field of electronics [13], considering that one of the highest concerns in graphene is to manipulate its electronic conduction, as an energy gap does not exist naturally. In short, such features arising from the inclusion of triple-bonded carbon linkages [14] are appealing for use in devices with exotic functionalities.

Up to now, scientists have already put in efforts to synthesize graphyne nanostructures and assembled subunits of them [15–17], but long-range, periodic structures have not been fabricated yet. However, promising results related to the large-area realization of other similar graphene allotropes, including triple-bonded carbon linkages, so-called graphdiyne films, and nanoribbons, have already been demonstrated [18, 19].

On the theoretical side, various groups have performed numerical characterizations to have an understanding of the electronic [10, 20–23], optical [24], mechanical [25–27], transport [28], thermal transport [29], and thermoelectric properties [30] of different graphyne structures, since the first suggestion of graphyne in 1987 [31]. Stability issues for α-graphyne have been discussed using phonon calculations and finite-temperature molecular dynamics simulations by V. Ongun Özçelik and colleagues [32]. However, a systematic and inclusive study of the vibrational and thermodynamic properties for the four different identified types of graphyne structures—α-, β-, γ- and 6, 6, 12-graphynes—is still missing in the literature. Considering the experimental efforts to synthesize these graphyne forms, understanding these physical properties is critical for stability issues.

With this intention, fundamental physical properties such as the electronic, vibrational, and thermodynamic characteristics of α-, β-, γ- and 6, 6, 12-graphyne are examined based on first-principles calculations in this research study. The obtained results for vibrational spectra, Grüneisen parameters (GPs), linear thermal expansion coefficients (LTECs), and Gibbs free energy as a function of temperature are presented with a comparison with those of graphene, which give clues to predict about the phase stability of these graphyne structures [33].

2. Theoretical methods

The *ab initio* calculations are performed using the Vienna Ab initio Simulation Package (VASP [34, 35]), which is based on density functional theory (DFT) [36]. The projector augmented wave pseudopotentials (PAW) [37, 38] from the standard distribution are incorporated into the calculations. For the electronic exchange-correlation functional, the generalized gradient approximation (GGA), in its Perdew–Burke–Ernzerhof parametrization [39], is used. The plane wave cut-off energy for all the materials are chosen as 500 eV. The Brillouin zone of α-, β-, γ-, and 6, 6, 12-graphyne are sampled with $14 \times 14 \times 1$, $12 \times 12 \times 1$, $14 \times 14 \times 1$, and $8 \times 12 \times 1$ Γ-centered k-points grids, respectively.

The vibrational properties of each structure are obtained by using PHONOPY [40] code, which can directly use the force constants calculated by density functional perturbation theory (DFPT) as implemented in the VASP code. Here, $2 \times 2 \times 1$ supercell structures are considered for all materials. The phonon mode Grüneisen parameters are calculated by using the equation

$$\gamma_{\nu}(\mathbf{q}) = -\left[\frac{a_0}{2\omega_{0,\nu}(\mathbf{q})}\right]\left[\frac{d\omega_{\nu}(\mathbf{q})}{da}\right], \tag{1}$$

where a_0 is the equilibrium lattice parameter, ω is the phonon frequency, ω_0 is the phonon frequency corresponding to the equilibrium structure, $\mathbf{q}$ is the Brillouin zone wave vector, and ν is the phonon mode index. The derivation of ω with respect to the lattice constant, a, (for 6, 6, 12-graphyne, the equilibrium b/a ratio is included to the calculations) is predicted by considering thee different structural parameters.

For α-, γ-, and 6, 6, 12-graphyne structures, the thermodynamic properties are predicted within the quasi-harmonic approximation (QHA) [41] in which temperature-dependent lattice parameters can be obtained by direct minimization of the Helmholtz free energy,

$$F(a_i, T) = (a_i) + \int\left[\frac{\hbar\omega^i}{2} + k_B T \times \int \ln\left(1 - \exp\left(-\frac{\hbar\omega^i}{k_B T}\right)\right)\right]\rho(\omega^i)d\omega^i, \tag{2}$$

where i is the structure index, $E(a_i)$ is the first-principles ground state energy of the structure i, ω is the phonon frequency, and $\rho(\omega^i)$ is the phonon density of states of the structure i. The dependence of the phonon frequencies on the lattice parameters is determined by calculating the phonon dispersions at 11 different lattice parameters, a_i (i = 1, 2, ... 11), around the first-principles equilibrium lattice constant of each material. Here, the lattice constant b_i of the anisotropic 6, 6, 12-graphyne structure is determined by using the calculated *ab initio* equilibrium b/a ratio for each a_i. The minimum Helmholtz free energies (Gibbs free energy, $G(T) = \mathrm{Min}\left[F(a_i, T)\right]$) and the corresponding lattice parameters are obtained by fitting the Birch–Murnaghan equation of states [42] to calculated Helmholtz free energy versus a_i for different temperatures, T (by 2 K temperature steps up to 1500 K). Finally, the linear thermal expansion coefficients (LTECs) of the materials are predicted as

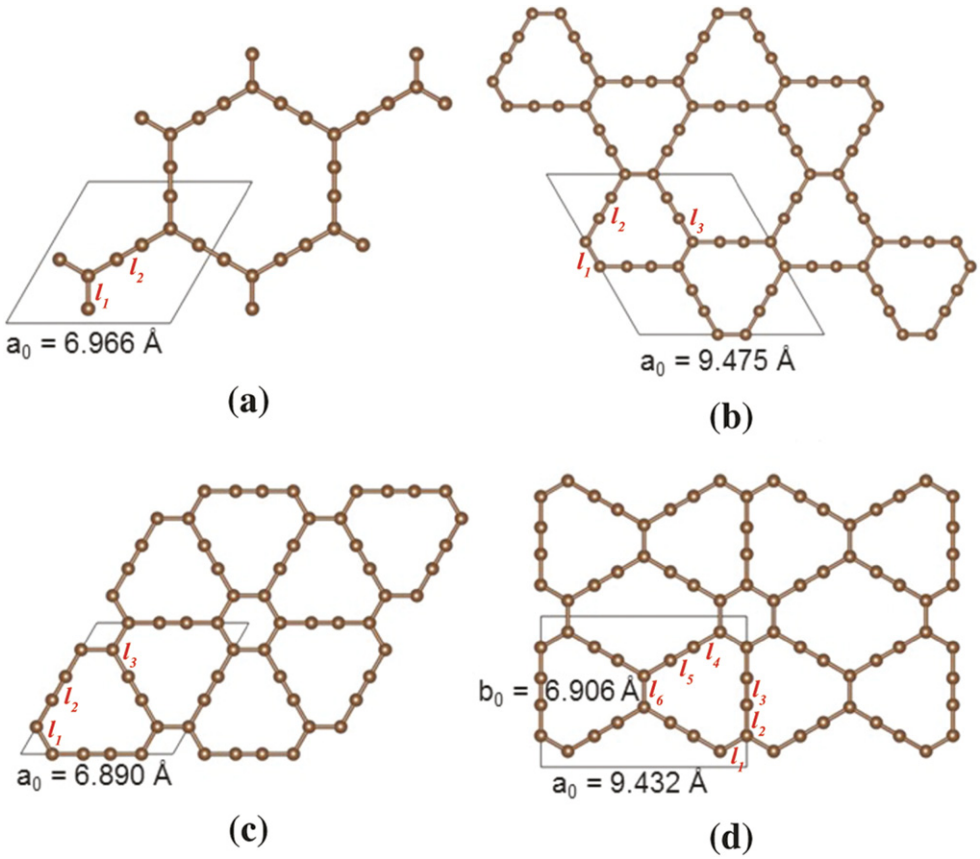

Figure 1. Schematic representations of (a) α-, (b) β-, (c) γ-, and (d) 6, 6, 12-graphyne. Quadrangles indicate unit cells. The depicted bond length values in Å are as follows: for α-graphyne $l_1 = 1.396$, and $l_2 = 1.230$, for β-graphyne $l_1 = 1.460$, $l_2 = 1.389$, and $l_3 = 1.232$, for γ-graphyne $l_1 = 1.426$, $l_2 = 1.408$, and $l_3 = 1.223$, and for 6,6,12-graphyne $l_1 = 1.426$, $l_2 = 1.409$, $l_3 = 1.224$, $l_4 = 1.398$, $l_5 = 1.227$, and $l_6 = 1.432$. Please see the supplementary material for the complete description of the lattices (available at stacks.iop.org/nano/25/185701/mmedia).

follows:

$$\alpha(T) = \frac{1}{a(T)}\frac{da(T)}{dT}, \tag{3}$$

where $a(T)$ is the equilibrium lattice parameter corresponding to the minimum Helmholtz free energy at any temperature.

3. Results and discussions

3.1. Electronic properties

Figure 1 shows the structures of, α-, β-, γ-, and 6, 6, 12 -graphyne, whose networks include single and triple bonds in addition to double bonds. The optimized first-principles lattice constants are also inserted on the schematic representations where these results are in agreement with other research works for α-, β-, and γ-graphyne [14, 20, 43]. Although the electronic properties of different graphyne allotropes have already been discussed in other studies, all of these four allotropes are not available in one specific report, and presenting each of them in one place is rather useful to compare the structures. Also, figure 2 is included to show the accuracy our results regarding the bandgaps and Fermi levels that could be confirmed easily. The hexagons in α-graphyne have been found to be equilateral, with a lattice constant of $a_0 = 6.966$ **Å** (figure 1(a)). For the case of β-graphyne (figure 1(b)), carbon triple bonds are placed into two-thirds of the C-C bonds in graphene, where the lattice constant is calculated as $a_0 = 9.475$ **Å**. As shown in figure 1(c), benzene rings are connected by carbon triple bonds and the lattice constant is calculated to be as $a_0 = 6.890$ **Å** for γ-graphyne. In addition to α-graphyne, both β- and γ-graphyne are hexagonally symmetric. However, for the case of 6, 6, 12-graphyne, the network shows rectangular symmetry and the lattice constants are determined as $a_0 = 9.432$ **Å** and $b_0 = 6.906$ **Å**, as presented in figure 1(d).

Figure 2 shows the calculated band structures of the four graphynes close to the Fermi energy. The electronic structures of the equilibrium lattice forms are in agreement with the results obtained by other reported studies [10, 13, 43, 44]. Similar to graphene, the electron and hole spectra of α-, β-, and 6, 6, 12-graphyne structures meet linearly at Dirac points in the momentum space. For the case of α-graphyne, the valance and conduction bands cross the Fermi level at K point; for β-graphyne, they cross on lines from Γ to M; and for 6, 6, 12-graphyne, they meet on the lines from Γ to X in addition to the lines from X' to M as shown in figures 2(a), (b), and (d), respectively. Different from α- and β-graphyne,

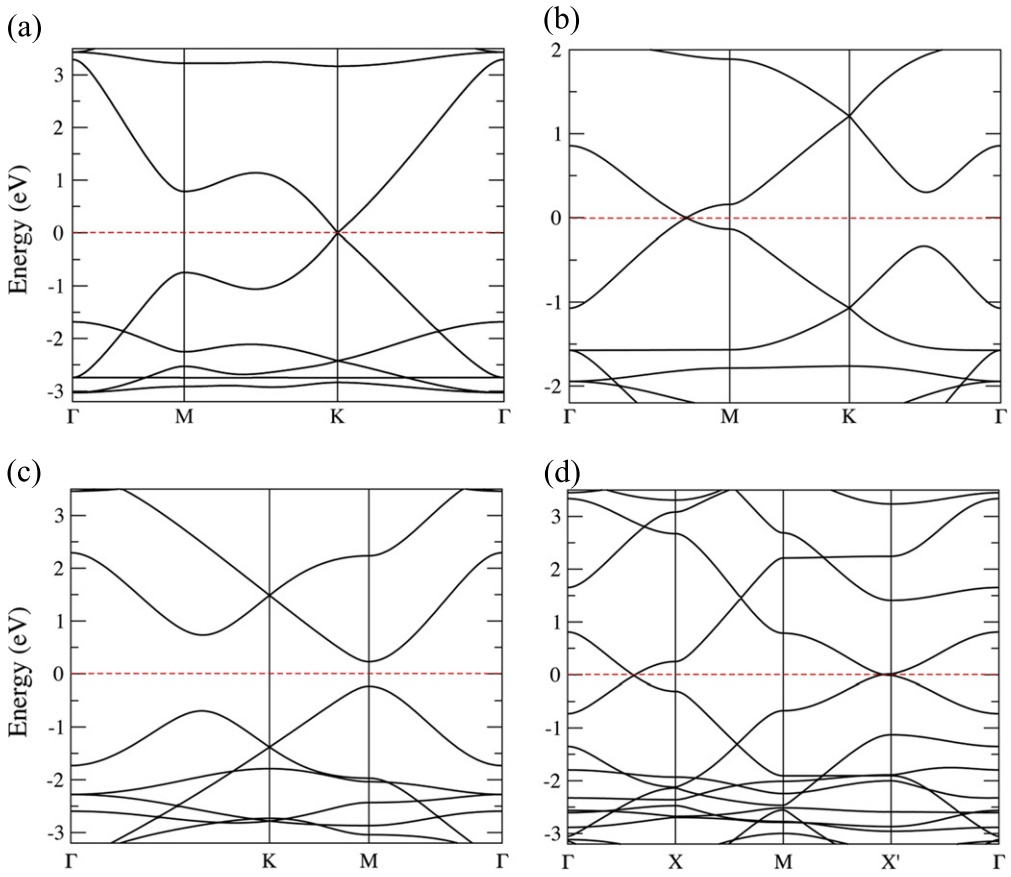

Figure 2. Electronic band structure of (a) α-, (b) β-, (c) γ-, and (d) 6, 6, 12-graphyne structures.

6, 6, 12-graphyne exhibits nonequivalent Dirac points with different curvatures [10]. This directional anisotropy results in direction-dependent electronic properties and hence adds a different potential to 6, 6, 12-graphyne for future applications. On the other hand, the electronic band structure of γ-graphyne exhibits a direct energy gap in the Brillouin zone at the M point, as displayed in figure 2(c). The calculated bandgap energy is around 0.5 eV, which is in accordance with the values obtained by other researches [11, 24, 43]. The distinct electronic structure of this form is explained by the Kekule distortion as a result of Peierls instability [14, 45] and indicates its potential particularly for optoelectronic applications.

3.2. Dynamical properties

Table 1 shows the Brillouin-zone-center phonon frequencies calculated using DFPT for the α-, β-, γ-, and 6, 6, 12-graphyne structures. The Raman-active zone-center optic phonon frequencies calculated using the nonorthogonal tight-binding (NTB) model [20] are also reported in the table for comparison purposes. Here, the underlined frequencies for α-, β-, and γ-graphyne structures represent the same Raman-active modes with the symmetries A_{1g} and E_{2g} (see Ref. [20] for the schematic representation of these zone-center modes). As expected, although the low-frequency values obtained using the NTB model are in close agreement with the ones that we calculated by DFPT, there is a deviation with increasing frequencies. According to the NTB model calculations [20], the atomic displacements of the Raman-active phonons are in-plane where α- and γ-graphyne show G-mode-like phonons at 30.339 and 45.508 THz, respectively. These values correspond to 30.425 and 42.356 THz, respectively, in our DFT calculations and lower than the G-band frequency of the graphene structure, 47.43 THz (1582 cm^{-1}). In β-graphyne, the frequency at 35.855 THz indicates motion of the carbon hexagons, and the frequency at 64.665 THz points to bond-stretching movements of the triple-bond atoms [20].

Figure 3 shows phonon dispersions for all of the defined graphyne structures. The calculated frequencies of all the modes for α-, γ-, and 6, 6, 12-graphyne networks are positive, and therefore there is no sign of low-temperature crystal instability of these networks. However, β-graphyne, whose negative modes of about −2 THz exist around the Γ point, shows low-temperature crystal instability due to its specific structure. Here, it is worth noting that systematic analysis of all the possible numerical and method related effects (plane wave cut-off energy, k-point grid, and lattice optimization criteria) that may cause imaginary frequencies at low-lying phonon modes has been performed. Due to the existence of imaginary frequencies, β-graphyne is excluded from further discussion since these imaginary frequency values do not allow us to apply QHA accurately to this material. All the graphyne networks exhibit rather flat phonon dispersions, specifically between 10 and 20 THz, and thus the phonon

Table 1. Brillouin-zone-center phonon frequencies (in THz) for α-, β-, γ-, and 6, 6, 12-graphyne. The underlined phonon frequencies indicate Raman-active phonon frequencies. The corresponding calculated Raman active phonon frequencies based on NTB model [20] are also listed.

α-graphyne		β-graphyne			γ-graphyne		6, 6, 12-graphyne		
0	16.590	0	12.504	25.815	0	19.917	0	12.901	29.406
0	16.590	0	12.504	25.815	0	19.917	0	13.541	31.082
0	18.264	0	13.587	30.225	0	22.925	0	14.053	32.606
5.482	18.863	2.960	13.587	33.804	5.277	23.085	2.892	14.599	35.228
6.663	30.425	2.960	13.611	34.306	5.277	27.637	3.142	15.498	36.375
6.722	30.425	3.378	13.870	34.306	6.892	27.637	3.716	15.670	39.279
6.722	30.557	3.378	14.042	38.012	6.892	30.978	4.624	15.838	40.251
11.938	43.222	4.257	15.772	42.756	7.492	30.978	5.950	15.974	40.517
13.413	43.222	4.955	15.772	42.756	9.977	34.918	6.513	16.200	42.107
13.413	60.287	8.381	16.362	43.604	12.165	39.720	7.342	19.086	43.027
15.706	60.287	8.456	16.362	43.604	12.344	42.356	8.925	19.838	43.416
15.706	66.854	8.456	18.394	45.888	12.344	42.356	9.999	19.918	43.702
		8.968	19.197	60.562	13.377	42.900	10.115	20.147	44.680
		9.035	19.838	60.562	14.753	43.406	10.675	20.663	63.164
		9.035	19.838	62.971	14.753	43.406	11.401	22.870	63.823
		10.291	19.919	63.729	16.018	64.880	11.538	23.087	64.716
		12.375	23.497	66.711	16.018	65.977	12.350	23.546	65.150
		12.375	23.497	66.711	19.870	65.977	12.644	27.224	67.210
Nonorthogonal tight-binding (NTB) Model [20]									
13.611	E_{2g}	7.285	E_{2g}		12.501	E_{2g}			
30.339	E_{2g}	12.411	A_{1g}		27.161	E_{2g}			
60.618	E_{2g}	13.910	E_{2g}		36.605	A_{1g}			
69.312	A_{1g}	23.624	E_{2g}		45.508	E_{2g}			
		34.866	E_{2g}		67.693	A_{1g}			
		35.855	A_{1g}		68.113	E_{2g}			
		44.010	E_{2g}						
		62.387	E_{2g}						
		64.665	A_{1g}						

transport and electron phonon coupling characters of graphyne structures might be rather different from those of graphene crystal.

The Grüneisen parameter is the physical indication of the shift in phonon frequencies when strain is applied to a material and can be calculated as follows:

$$\gamma_v(\mathbf{q}) = \left[\frac{a}{2\omega_v(\mathbf{q})}\right]\left[\frac{d\omega_v(\mathbf{q})}{da}\right]. \quad (4)$$

For these novel material networks, once the GPs are identified, phonon monitoring by Raman spectroscopy would allow the detection of strain as the amount of the shift of phonon frequencies with strain is proportional to these GPs, which are also indicative of thermomechanical properties [46–48]. Figure 4 presents the calculated GPs along the high-symmetry directions in the Brillouin zone of the materials. The GP values of three acoustic modes are considerably negative for all the graphyne forms. Besides, negative GP values as low as −8 were calculated for low-lying optical modes of all of the networks. However, the mode GPs of the graphene structure shows notable negative behavior only for the first acoustic mode [49]. The zone-center GP values corresponding to the first acoustic mode of α- and 6, 6, 12-graphyne structures are comparable with those of graphene [49] (∼−80), where this value for γ-graphyne is smaller than −400.

3.3. Thermal properties

The calculated LTECs for graphene and the α-, γ-, and 6, 6, 12 -graphyne structures as a function temperature are shown in figure 5. The LTECs for graphene calculated by Mounet *et al* are also included in the figure for comparison. [49]. These graphene results are in quite good agreement with our calculations up to high temperatures. While the curves of graphyne structures follow a similar trend to those of graphene, the magnitude of the negative coefficients are slightly lower for temperatures higher than 500 K. For the γ- and, specifically, 6, 6, 12-graphyne structures, the LTECs are calculated to be more negative at low temperatures. Due to the quadratic nature of 6, 6, 12-graphyne, LTEC in the direction of b is nearly twice higher in magnitude than the case of a, showing direction-dependent expansion. However, it is important to mention that distinctively for this material, QHA calculations are performed with 11 different unit cell areas ($b \times a$) considering the first principle b/a ratio that we calculated using DFT as an inset in figure 5. The predicted large thermal contraction for all the graphyne forms are in correlation with the GPs shown in

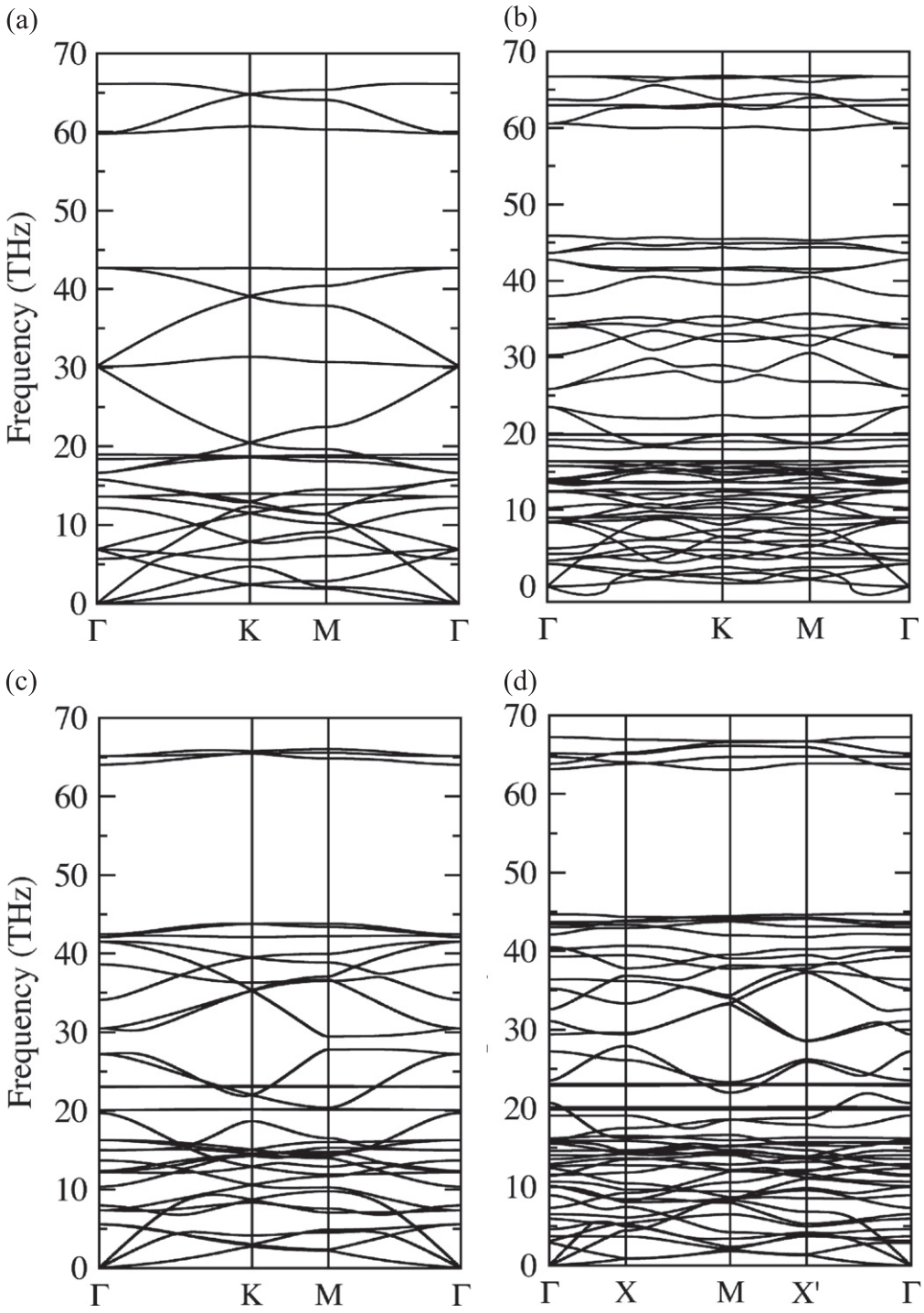

Figure 3. Calculated phonon dispersions for (a) α-, (b) β-, (c) γ-, and (d) 6, 6, 12-graphyne.

figure 4. Indeed, the large negative Grüneisen parameters of acoustic modes give rise to negative LTEC [50] in particular at low temperatures. One other important quantity, particularly for device application of these materials, is the negative-to-positive transition of LTEC. Our QHA calculations yield that the transition temperatures of all the materials are remarkably higher than the room temperature, 620 K for α-graphyne structures, 1150 K for γ-graphyne structures, and 1550 K for 6, 6, 12-graphyne structures.

Finally, Gibbs free energy values per atom are calculated when pressure is kept constant and the temperature is changed. Determining the lowest Gibbs free energy as a function of temperature gives information on which phase is more stable at a specific temperature. Up to now, there have been different studies on Gibbs free energy minimization for determining phase equilibrium [51–53]. Hence, it is an important parameter to assess the thermodynamic phase stability of different networks and allows us to predict the direction of change for a system under the

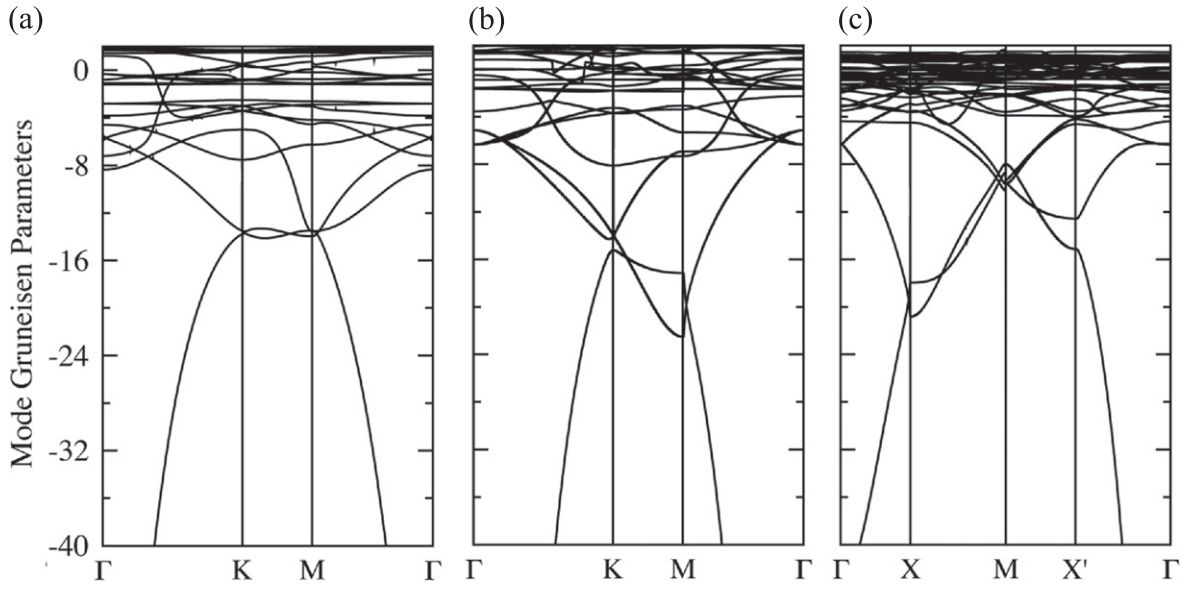

Figure 4. Calculated Grüneisen parameters for (a) α-, (b) γ-, and (c) 6, 6, 12-graphyne.

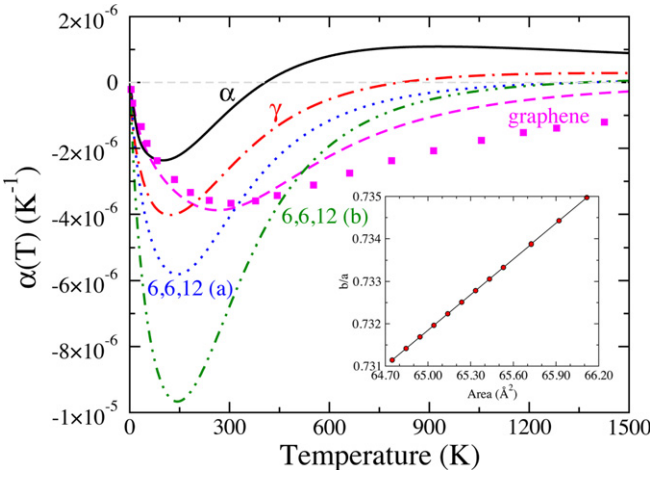

Figure 5. Lattice thermal expansion coefficients for α-, γ-, and 6, 6, 12-graphyne and graphene structures. The magenta square dots shows the LTEC of graphene reported by Mounet *et al* [49]. The inset shows the change in the ratio of lattice constants for 6, 6, 12 -graphyne as the area is increased.

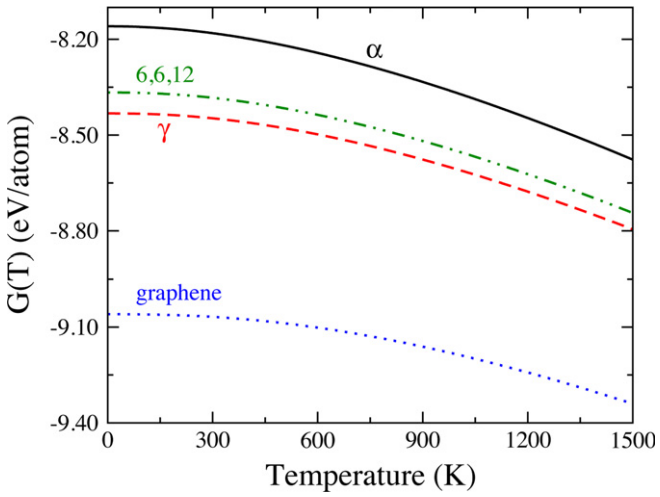

Figure 6. Gibbs free energy, $G(T)$, for graphene and α-, γ-, and 6, 6, 12-graphyne structures.

constraints of constant temperature and pressure where eventually these calculations are crucial for simulation and optimization of chemical processes [54]. Figure 6 displays the calculated Gibbs free energy $\left(G(T) = \mathrm{Min}\left[F\left(\{a_i\}T\right)\right]\right)$ per atom results for graphene and α-, γ-, and 6, 6, 12-graphyne structures. When the excess of binding energies per atom of the graphynes with respect to graphene is calculated at 0 K, they are found to be 0.90 eV, 0.85, 0.63, and 0.69 eV for α-, β-, γ-, and 6, 6, 12-graphyne structures, respectively. These results are in agreement with the results determined by Popov *et al* [20] (0.96, 0.87, and 0.63 eV for α-, β-, and γ-graphyne structures). These differences remain nearly constant even if we increase the temperature up to 1500 K. The results could indicate a relatively lower phase stability for the graphyne networks when compared to graphene by a difference of at least 500 meV/atom up to 1500 K.

4. Conclusion

In summary, a systematic study of the vibrational and thermodynamic properties of the graphene-related structures of α-, β-, γ-, and 6, 6, 12-graphyne are presented. The DFPT calculations show that no imaginary frequencies exist in α-, γ-, and 6, 6, 12-graphyne networks. However, negative modes of about −2 THz are predicted around the Γ point for β-graphyne structures, which points out the low-temperature crystal instability of this network. Furthermore, the obtained negative GPs particularly for the acoustic and low-laying

optical modes of these structures reveal the length contraction in these graphyne networks with increase in temperature. Indeed, QHA simulations regarding the LTEC calculations exhibit a higher negative behavior in comparison with graphene. Additionally, the $G(T)$ calculations, which do not take into account the anharmonic effects, reveal that large-area growth would not be straightforward for these graphene allotropes including triple-bonded carbon linkages.

Acknowledgments

We would like to thank the ULAKBIM High Performance and Grid Computing Center for a sufficient time allocation for our projects. CS particularly acknowledges the support from the Scientific and Technological Research Council of Turkey (TUBITAK 113F096) and Anadolu University (BAP-1306F261) for this project. NKP particularly acknowledges the support from Anadolu University (BAP-1306F174) for this project.

References

[1] Novoselov K, Geim A, Morozov S, Jiang D, Zhang Y, Dubonos S, Grigorieva I and Firsov A 2004 *Science* **306** 666
[2] Haskins J, Kinaci A, Sevik C, Sevinçli H, Cuniberti G and Çağın T 2011 *ACS Nano* **5** 3779
[3] Bonaccorso F, Sun Z, Hasan T and Ferrari A C 2010 *Nat. Photonics* **4** 611
[4] Schwierz F 2010 *Nat. Nanotechnol.* **5** 487
[5] Allen M J, Tung V C and Kaner R B 2010 *Chem. Rev.* **110** 132
[6] Boukhvalov D W and Katsnelson M I 2009 *J. Phys. Condense Mat.* **21** 344205
[7] Sevinçli H, Sevik C, Çağın T and Cuniberti G 2013 *Sci. Rep.* **3** 1228
[8] Enyashin A N and Ivanovskii A L 2011 *Phys. Stat. Sol* B **248** 1879
[9] Lusk M T and Carr L D 2009 *Carbon* **47** 2226
[10] Malko D, Neiss C, Vi nes F and Görling A 2012 *Phys. Rev. Lett.* **108** 086804
[11] Narita N, Nagai S, Suzuki S and Nakao K 1998 *Phys. Rev.* B **58** 11009
[12] Kondo M, Nozaki D, Tachibana M, Yumura T and Yoshizawa K 2005 *Chem. Phys.* **312** 289
[13] Zhou J, Lv K, Wang Q, Chen X S, Sun Q and Jena P 2011 *J. Chem. Phys.* **134** 174701
[14] Kim B G and Choi H J 2012 *Phys. Rev.* B **86** 115435
[15] Haley M M 2008 *Pure Appl. Chem.* **80** 519
[16] Spitler E L, Johnson C A II and Haley M M 2006 *Chem. Rev.* **106** 5344
[17] Takeda T, Fix A G and Haley M M 2010 *Org. Lett.* **12** 3824
[18] Qian X, Ning Z, Li Y, Liu H, Ouyang C, Chen Q and Li Y 2012 *Dalton T.* **41** 730
[19] Li G, Li Y, Liu H, Guo Y, Li Y and Zhu D 2010 *Chem. Commun.* **46** 3256
[20] Popov V N and Lambin P 2013 *Phys. Rev.* B **88** 075427
[21] Lu H and Li S D 2013 *J. Mater. Chem.* C **1** 3677
[22] Özçelik V O and Ciraci S 2013 *J. Phys. Chem.* C **117** 2175
[23] Liu Z, Yu G, Yao H, Liu L, Jiang L and Zheng Y 2012 *New J. Phys.* **14** 113007
[24] Kang J, Li J, Wu F, Li S S and Xia J B 2011 *J. Phys. Chem.* C **115** 20466
[25] Cranford S W and Buehler M J 2011 *Carbon* **49** 4111
[26] Zhang Y Y, Pei Q X and Wang C M 2012 *Appl. Phys. Lett.* **101** 081909
[27] Ajori S, Ansari R and Mirnezhad M 2013 *Mater. Sci. Eng.:* A **561** 34
[28] Ni Y, Yao K L, Fu H H, Gao G Y, Zhu S C, Luo B, Wang S L and Li R X 2013 *Nanoscale* **5** 4468
[29] Ouyang T, Chen Y, Liu L M, Xie Y, Wei X and Zhong J 2012 *Phys. Rev.* B **85** 235436
[30] Wang X M, Mo D C and Lu S S 2013 *J. Chem. Phys.* **138** 204704
[31] Baughman R H, Eckhardt H and Kertesz M 1987 *J. Chem. Phys.* **87** 6687
[32] Özçelik V O and Ciraci S 2013 *J. Phys. Chem.* C **117** 2175–82
[33] Palciauskas V 1975 *J. Phys. Chem. Solids* **36** 611
[34] Kresse G and Hafner J 1993 *Phys. Rev.* B **47** 558
[35] Kresse G and Furthmüller J 1996 *Phys. Rev.* B **54** 11169
[36] Martin R M 2004 *Electronic Structure* (Cambridge: Cambridge University Press)
[37] Blöchl P E 1994 *Phys. Rev.* B **50** 17953
[38] Kresse G and Joubert D 1999 *Phys. Rev.* B **59** 1758
[39] Perdew J P, Burke K and Ernzerhof M 1996 *Phys. Rev. Lett.* **77** 3865
[40] Togo A, Oba F and Tanaka I 2008 *Phys. Rev.* B **78** 134106
[41] Pavone P, Karch K, Schütt O, Strauch D, Windl W, Giannozzi P and Baroni S 1993 *Phys. Rev.* B **48** 3156
[42] Birch F 1947 *Phys. Rev.* **71** 809
[43] Wu W, Guo W and Zeng X C 2013 *Nanoscale* **5** 9264
[44] Yang P and Hai-Bin W 2013 *Chinese Phys.* B **22** 057303
[45] Lee S H, Chung H J, Heo J, Yang H, Shin J, Chung U I and Seo S 2011 *ACS Nano* **5** 2964
[46] Ferrari A C 2007 *Solid. State. Commun.* **143** 47
[47] Mohiuddin T M G *et al* 2009 *Phys. Rev.* B **79** 205433
[48] Grimvall G 1986 *Thermophysical Properties of Materials* (Amsterdam: North-Holland)
[49] Mounet N and Marzari N 2005 *Phys. Rev.* B **71** 205214
[50] Barron T, Collins J and White G 1980 *Adv. Phys.* **29** 609
[51] Tessier S R, Brennecke J F and Stadtherr M A 2000 *Chem. Eng. Sci.* **55** 1785
[52] Castillo J and Grossmann I E 1981 *Comput. Chem. Eng.* **5** 99
[53] Rossi C, Cardozo-Filho L and Guirardello R 2009 *Fluid Phase Equilib.* **278** 117
[54] Teh Y and Rangaiah G 2002 *Chem. Eng. Res. Des.* **80** 745